

# EFFECT OF THE SINTERING PROCESS ON THE MORPHOLOGY AND MECHANICAL PROPERTIES OF $\text{La}_{0.6}\text{Sr}_{0.4}\text{Co}_{0.2}\text{Fe}_{0.8}\text{O}_{3-\delta}$ ASYMMETRIC FLAT MEMBRANES PREPARED BY THE PHASE INVERSION METHOD

SILVANA DWI NURHERDIANA, RIFKA ETRIANA, RENDY MUHAMAD IQBAL,  
WAHYU PRASETYO UTOMO, #HAMZAH FANSURI

*Department of Chemistry, Faculty of Science, Institut Teknologi Sepuluh Nopember (ITS),  
Kampus ITS Sukolilo, Surabaya 60111, Indonesia*

#E-mail: [h.fansuri@chem.its.ac.id](mailto:h.fansuri@chem.its.ac.id)

Submitted November 24, 2018; accepted May 27, 2019

**Keywords:** Perovskite oxide  $\text{La}_{0.6}\text{Sr}_{0.4}\text{Co}_{0.2}\text{Fe}_{0.8}\text{O}_{3-\delta}$ , Phase inversion, Asymmetric membrane, Sintering temperature

*The goal of this study was to understand the effect of sintering temperature and duration on the morphology and mechanical properties of the  $\text{La}_{0.6}\text{Sr}_{0.4}\text{Co}_{0.2}\text{Fe}_{0.8}\text{O}_{3-\delta}$  (LSCF) asymmetric flat membrane. The LSCF was prepared using the solid-state method and flat asymmetric membranes were prepared from LSCF powder using polyethersulfone (PESf) as the binder, dimethyl sulfoxide (DMSO) as the solvent and demineralized water as the coagulant (non-solvent). The membranes were sintered at 950, 1100, and 1250 °C for 4 and 8 h to examine the effect of sintering temperature on the morphology, porosity, hardness and thermal expansion properties of the resulting membranes. Analysis of the results showed a slight difference in membrane density when employing a sintering duration of 4 and 8 h at the same temperature. Whilst sintering temperature was observed to significantly affect the morphology and mechanical properties of the asymmetric membrane. SEM images showed that all membranes retained their asymmetric structure with finger-like pores in their porous layer. Increasing the sintering temperature produced greater membrane density, where sintering at 1250 °C produced the strongest membrane with the greatest density and hardness (412.36 Hv). The thermal expansion of the membranes was also measured by TMA, which demonstrated a low thermal expansion coefficient associated with the denser membranes.*

## INTRODUCTION

Membrane technology has been widely used for separation processes. One membrane type that has been developed as an oxygen separator and catalyst are inorganic ceramic membranes. One example of such ceramic membrane materials with promising characteristics are those derived from the perovskite oxide families, due to the specific Mixed Ionic and Electronic Conductor (MIEC) characteristics associated with the perovskite structure. These oxides have the ability to release lattice oxygen without causing significant structural changes in the crystal lattice [1]. Therefore, the MIEC membrane has the potential to be used for applications such as functioning as a selective oxygen supplier for partial oxidation of the methane (POM) reaction and for solid oxide fuel cells (SOFC) [2].

Among the perovskite oxide families, lanthanum-based perovskites, such as  $\text{La}_{0.6}\text{Sr}_{0.4}\text{Co}_{0.2}\text{Fe}_{0.8}\text{O}_{3\delta}$  (LSCF) show high oxygen permeability characteristics [3-6]. However, the oxygen permeability of these materials needs to be improved to be able to be applied to commer-

cial applications. Improving oxygen permeability may be achieved by preparing the material upon an asymmetric membrane, which consists of a very thin but dense layer located on a thicker, porous support. The microstructure of the asymmetric membrane also provides additional mechanical strength to the dense layer [7].

Phase inversion, followed by sintering, is one method that can be used to prepare an asymmetric LSCF membrane. The phase inversion method is a process by which polymers in a solution coagulate and change phase from liquid to solid when the solvent is displaced by a non solvent. The coagulation process is influenced by several factors, such as the nature of the polymer, the type of solvent and non-solvent, the viscosity of the polymer solution, and the sintering temperature applied during the process [8].

Tan et al. [9] reported the fabrication of a LSCF asymmetric membrane employing polyethersulfone (PESf) as the polymer binder to form the asymmetric structure, whereby the resulting membrane exhibited good mechanical strength. Setyaningsih et al. [10] reported that polyetherimide (PEI) could also be used as the

polymer binder in the preparation of the asymmetric CaTiO<sub>3</sub> membrane. However, the membrane was very fragile due to low membrane density and the membrane morphology changed significantly before and after sintering. Whilst the pre-sintered membrane showed well-formed, finger-like pores, the pores became irregular after sintering. It was assumed that the change was caused by very rapid polymer decomposition occurring during the sintering process.

The sintering process and its effect on the mechanical properties of the Ba<sub>x</sub>Sr<sub>1-x</sub>Co<sub>0.8</sub>Fe<sub>0.2</sub>O<sub>3-δ</sub> (BSCF) membrane were also studied in detail by Fansuri et al. [11]. It was found that the sintering process could lead to shrinkage of the membrane and increase the membrane's density. A sintering process found to be inappropriate is a direct process whereby the temperature is raised rapidly from room temperature to the final sintering temperature. Rapid temperature increases can create cracks on the membrane due to thermal shock. This cracking can be minimized by a step-by-step sintering process, which gives sufficient time for the membrane to decompose its organic and volatile matter before being subjected to the final sintering step at an increased temperature. This can be achieved by employing a sintering process that is subjected to some holding at certain temperatures prior to elevation to the final temperature. This procedure may function to reduce thermal shock and retain the original shape of the sintered membranes. Furthermore, the final sintering temperature may also affect the morphology and characteristics of the membrane.

Utomo et al. [12] reported that the optimal final sintering temperature was mainly determined by the composition of the perovskite. With the composition which was studied by the Utomo et al., when the sintering temperature was too low, the density of the membrane is also too low. On the other hand, when the temperature was too high, the membrane melted. The melting damaged the asymmetric structure of the membrane as the particles from the dense layers melted down into the porous layer, creating holes in the dense layer and causing pore formations on the dense layer. In addition, for an asymmetric membrane prepared by the phase inversion method, the polymer removal during the sintering process should be carried out cautiously to avoid pore structure damage [13].

Based on previous research, it is suggested that the sintering stage is one of the main factors that influences the formation of the asymmetric dense membrane. Sintering temperatures may affect the final product of the membrane in terms of morphology and its mechanical properties. Therefore, the work of this study was aimed at obtaining a deeper understanding of the effect of sintering temperature on the LSCF asymmetric membrane prepared by the phase inversion method. The membrane density, as well as its morphology and mechanical properties, especially membrane hardness and thermal coefficient, are discussed below.

## EXPERIMENTAL

### Materials

The materials used for synthesis of LSCF were lanthanum oxide (La<sub>2</sub>O<sub>3</sub>) 99.5 % (Merck), strontium carbonate (SrCO<sub>3</sub>) 99.9 % (Merck), cobalt oxide (Co<sub>3</sub>O<sub>4</sub>) 99.5 % (Merck) and iron oxide (Fe<sub>2</sub>O<sub>3</sub>) > 97 % (UPT BPPTK LIPI). The materials were used directly without any pre-treatment and any further purification. Preparation of the asymmetric membrane was carried out using polyethersulfone (PESf) as the polymer binder, dimethylsulfoxide (DMSO) as the solvent and demineralized water (DM water) as the non-solvent.

### Methods

#### *Synthesis of LSCF 6428*

La<sub>0.6</sub>Sr<sub>0.4</sub>Co<sub>0.2</sub>Fe<sub>0.8</sub>O<sub>3-δ</sub> (LSCF 6428) was synthesized using solid-state methods as reported by Setyaningsih et al. [10] and Nurherdiana et al. [14]. Before starting the synthesis, all reactants were dried in an oven at 105 °C for 1 h. After drying, the materials were left to cool to room temperature inside a desiccator. The dried reactants were weighed according to their stoichiometric compositions. After weighing, the stoichiometric amounts of La<sub>2</sub>O<sub>3</sub> (0.3 mole), SrCO<sub>3</sub> (0.4 mole), Co<sub>3</sub>O<sub>4</sub> (0.067 mole), and Fe<sub>2</sub>O<sub>3</sub> (0.4 mole) were then mixed and ground for 2 h until homogeneous. The powdered mixture was then subject to calcination at 1000 °C for 2 h with an increasing temperature rate of 3 °C·min<sup>-1</sup>. The calcination process was repeated twice with intermediate grinding to improve the formation rate of LSCF perovskites. After calcination, the product was then ground again for 15 minutes and sieved using a 400-mesh test sieve (particle size ≤ 45 μm). The resulting powder was then characterized by an X-ray Diffractometer (XRD JEOL JDX-3530) using Cu Kα radiation (λ = 1.5406 Å). The measurement was performed at 2θ = 20-90° with a speed of 0.5°·min<sup>-1</sup> and 0.02° step size.

#### *Preparation of the asymmetric membrane*

The asymmetric membrane of LSCF was prepared by the phase inversion method as reported by Wang et al. [15]. The composition of reactants (in wt. %) was 5.23 % PESf, 42.66 % DMSO and 53.11 % LSCF as a fine powder. The mixture was made by placing DMSO into a conical flask followed by pouring the LSCF into the flask. The conical flask was then closed and the mixture was stirred using a magnetic stirrer for 2 h until a homogeneous slurry was formed. PESf pellets were then gradually added into the stirred slurry and the mixture was continuously stirred for another 48 h to allow the polymer solution and perovskite powder to blend and form a homogeneous suspension. The suspension was then poured directly onto a glass plate and levelled, and

directly immersed into a bath containing DM water. The resulting green membrane was cut into a  $17.0 \times 17.0$  mm square and sintered at various temperatures (950, 1100 or 1250 °C).

The shrinkage of the membranes after sintering was calculated based on the difference in the membrane's length ( $l$ ), before and after sintering as shown in Equation 1. The porosity of the membrane was measured approximately based on the volume of water that could be absorbed onto the membrane. For this purpose, the dry membrane was weighed initially and then immersed in warm water (40 °C) for 15 min to wet the membrane. The membrane was then taken out of the warm water and excess water on its surface was carefully wiped off. The mass of adsorbed water was determined from the weight difference between the dry and wet membrane. The mass difference indicated the mass of water adsorbed, and by using water density data, the volume of adsorbed water could be calculated. The porosity was calculated per gram of the initial membrane using Equation 2.

$$\text{Shrinkage (\%)} = \frac{l_{\text{initial}} - l_{\text{final}}}{l_{\text{initial}}} \quad (1)$$

$$\text{Porosity} \left( \frac{\text{mL}}{\text{g}} \right) = \frac{m_2 - m_1/\rho}{m_1} \quad (2)$$

where  $m_1$  is the mass of the dry membrane (in g),  $m_2$  is the mass of wet membranes (in g) and  $\rho$  is the density of water ( $1 \text{ g}\cdot\text{ml}^{-1}$ ).

The surface and cross-section of the green membranes before and after sintering were examined by Scanning Electron Microscope (SEM) ZEISS EVO MA 10 with an accelerating voltage of 20.00 kV using a Secondary Electron (SE) detector. Carbon coating was applied to the sample before SEM analyses to improve the electrical conductivity of the samples. Thermal decomposition of the green membrane was analyzed by Mettler-Teledo TGA-DSC 1 at temperatures ranging from room temperature to 1000 °C in air with an increasing temperature rate of  $10 \text{ }^\circ\text{C}\cdot\text{min}^{-1}$ . The membrane hardness was characterized by MITUTOYO type 211 Micro Vickers Hardness Tester with a 0.2 kgF indentation force and was retained for 10 s at 5 different points on the membrane's surface. The thermal expansion coefficient of the membranes was characterized by METLER TOLEDO TMA/SDTA 840 measured in the range from room temperature to 1000 °C with an increasing temperature rate of  $10 \text{ }^\circ\text{C}\cdot\text{min}^{-1}$  and load of 0.02 N.

Table 1. Database for refinement of LSCF 6428.

PDF No.	Space group	Lattice
00-049-0284	R - 3 C : H	Trigonal [Hex]
00-086-1665	R - 3 C : R	Trigonal [Rh]

## RESULTS AND DISCUSSION

### Synthesis of LSCF 6428

The solid-state method was used to synthesize the fine LSCF perovskite powder where the apparent change in powder color from red to black was an indicator of the phase change from metal oxides and carbonates to the perovskite oxide. The crystal structure of the powder was then characterized using X-ray diffraction to confirm the formation of the perovskite structure. Figure 1 shows the diffractogram of the LSCF fine powder, which is consistent with the diffractogram of the LSCF 6428 (PDF No. 049-0285) standard, demonstrating that perovskite oxides were successfully formed using this method. The absence of additional peaks showed that there was no other phase beside the perovskites present. The X-ray diffractogram also exhibited sharp and intense peaks as an indication of high crystallinity of the resulting perovskite oxide.

To obtain additional data, the diffractogram was further analyzed by the Rietveld refinement method using Rietica™ software. When a single LSCF 6428 phase (using model of PDF No. 00-049-0284) was used as the input file, there were some very clear residual peaks as shown in Figure 1b.

Further investigation using search & match software with a JCPDS database shows the possibility of a second phase similar to the  $\text{LaCoO}_3$  structure, which possesses symmetry similar to LSCF 6428. Therefore, the diffractogram was refined by adding a  $\text{LaCoO}_3$  structural model (PDF No. 00-086-1665) as the second phase. Table 1 shows the crystal models that were used as input data for the refinement. By using this data, the results were consistent with the diffraction data shown in Figure 1c where  $R_p = 6.04$ ,  $R_{wp} = 7.61$  and the goodness of fit ( $\chi^2$ ) was 1.38. The weight percentages of the phases were 56.41 and 43.59 for the LSCF 6428 and  $\text{LaCoO}_3$ .

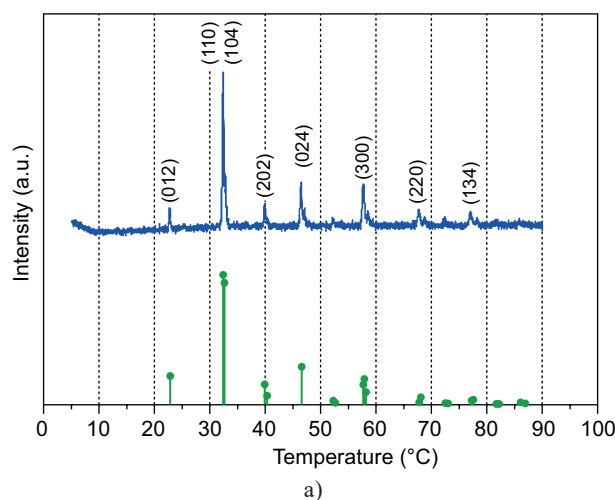


Figure 1. XRD pattern of LSCF 6428 (a). (Continue on next page)

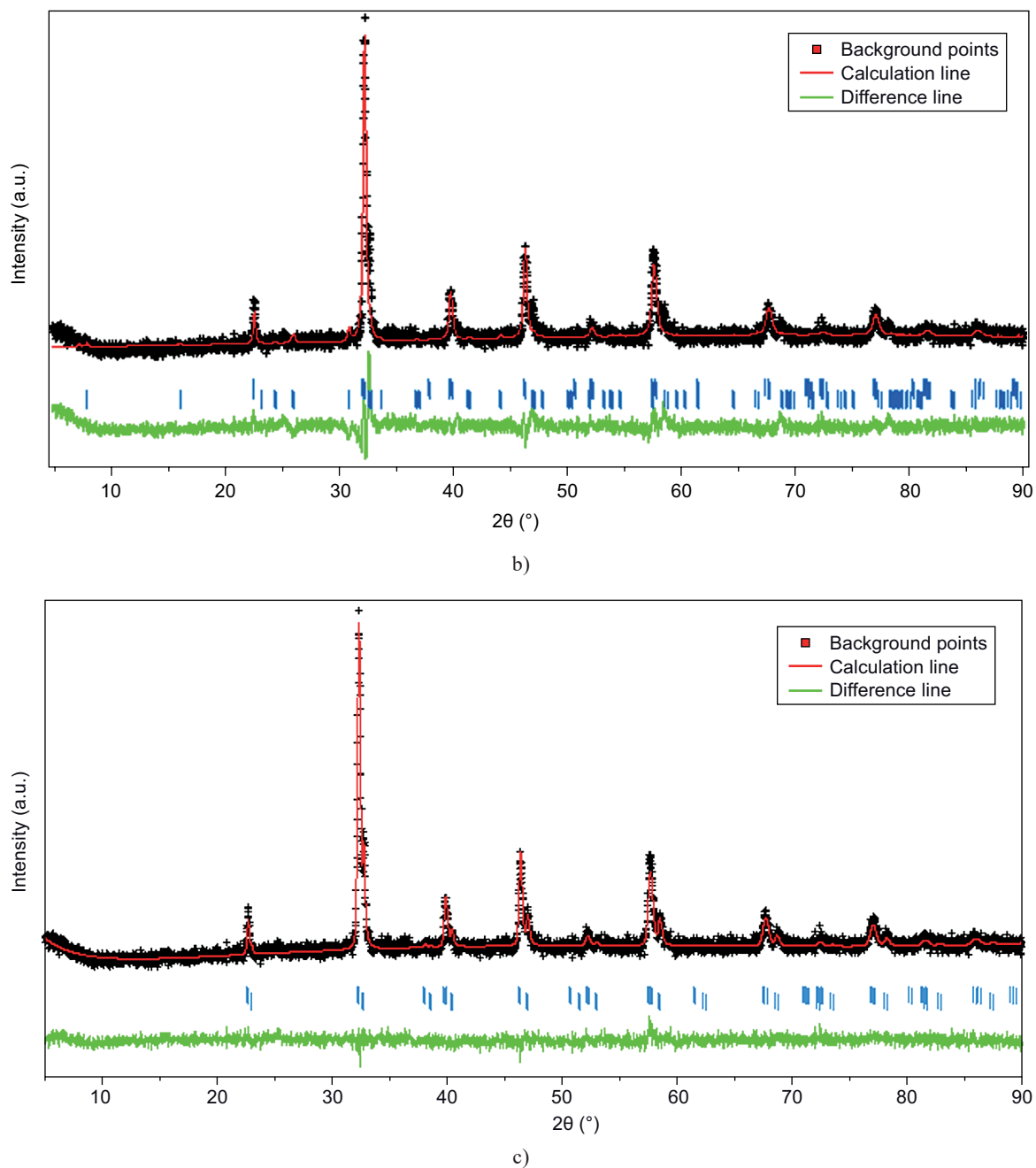


Figure 1. The refinement result using single LSCF 6428 (b) and a combination of LSCF 6428 and LaCoO<sub>3</sub> structure data input (c).

Table 2. Lattice parameters of refined structure.

Space group	a (Å)	b (Å)	c (Å)	$\alpha$ (°)	$\beta$ (°)	$\gamma$ (°)	Lattice volume (Å <sup>3</sup> )
R-3 C :H	5.5443	5.5443	13.5241	90	90	120	360.0248
R-3 C :R	5.4655	5.4655	5.4655	59.98	59.98	59.98	115.3953

structures, respectively. In addition, the derived bragg R-factors (%) were 3.03 for LSCF 6428 and 1.49 for LaCoO<sub>3</sub>. The refined unit cell parameters are listed in Table 2.

The measured lattice size of the R-3C:R cube phase was slightly lower than that reported by Mineshige et al. [16], where the authors reported that the length of

the lattice ( $a = b = c$ ) was 5.468 Å, which increased when there were more Sr deficiencies. The smaller size observed in this study, therefore indicates that the resulting LSCF 6428 has a low Sr deficiency.

The existence of two similar lattice structures was also reported by other researchers such as Hjalmarrsson et al. [17] and Kivi et al. [18] who reported LSCF 6426 with

a rhombohedral R-3C:R space group while Hashimoto et al. [19] reported a trigonal structure. However, all previous reports show a slightly smaller unit cell size than the results obtained through this research.

#### Preparation of asymmetric membranes

Asymmetric membranes were prepared by the phase inversion method. The method was chosen because of its ability to produce membranes with various asymmetric structures as well as the relative simplicity of the process [15]. In asymmetric dense membranes, there are two layers, namely the dense and porous layers. The thickness of the dense layers should be as thin as possible, whereas the porous layer should be thicker and have finger-like pores. The finger-like pores integrate the sponge-like pores in the microstructure of the membrane, which initiates enhancement of oxygen ion diffusion, as described elsewhere [12].

The suspension was first prepared using DMSO as the solvent, which has the ability to dissolve PESf and is soluble in the non-solvent (DM water) [13]. The suspension was then poured onto a glass plate. The thickness of the membrane was maintained at  $\pm 2$  mm and directly transferred to a coagulant bath containing DM water. In this process, the DMSO was dissolved in water, where the water exchanges with the DMSO causing the polymer to change from the liquid to the solid phase. The exchange of DMSO with water facilitated the creation of pores during the immersion

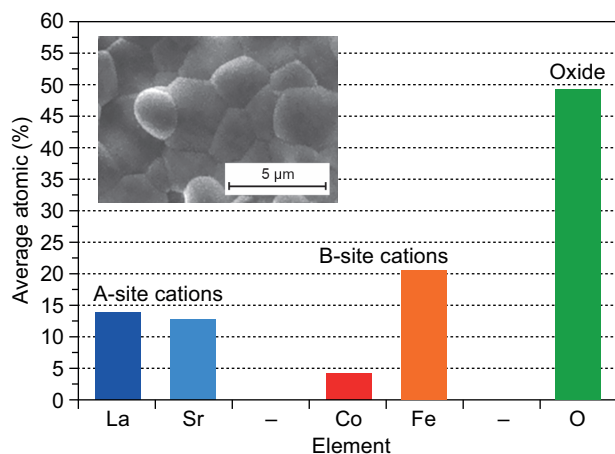


Figure 2. EDX elemental compositions of sintered LSCF 6428 membrane at 1250 °C.

Table 3. Element ratio of the A and B site cations in LSCF 6428 membrane.

The site of cations	Elements ratio	Theory	Experiment
A	La/Sr	1.5	1.1
B	Co/Fe	0.25	0.21

process. As the solvent is exchanged within the polymer solution with the demineralized water, the polymer is coagulated, resulting in a membrane of increased density with a certain pore structures as reported by Yuan et al. [20]. The membrane is then immersed for 24 h prior to sintering.

Chemical analysis was carried out to determine the composition of LSCF 6428 in the flat membrane using SEM-EDX at several analysis points. According to Figure 2, the LSCF 6428 membrane contains different average atomic percentages of La, Sr, Co, Fe and O. The elemental composition ratios for each analysis site is shown in Table 3. The calculation of the element ratios theoretically did not vary significantly from the experimental results, which confirmed that there was no significant change in the composition of LSCF 6428 in the membrane form. In addition, this also supports the XRD result that LSCF 6428 was successfully synthesized using the precursors and methods carried out in previous studies.

The green membrane obtained from the phase inversion method was then analyzed by TGA to determine the effect of the sintering process. The TGA curve was divided into five weight loss steps as shown in Figure 3. The first (I) step ranging from room temperature to 500 °C was assigned as the step relating to the removal of any physically adsorbed water and residual solvent that might exist in the membranes [20]. Previous researchers have reported that the pure PESf membrane would decompose directly at temperatures between 500 and 600 °C [9, 20, 21, 22, 23]. Thus, the second (II) step ranging from 500-600 °C was attributed to the decomposition of the PESf polymer. However, the proportion of weight lost in this step (3.86 %) is much less than the calculated theoretical proportion (9.12 %) based on the weights of PESf and LSCF when DMSO was excluded. The result shows that not all of the PESf was directly decomposed into  $CO_2$ ,  $SO_x$  and  $H_2O$  in step II when exposed to the air atmosphere.

The weight loss was continuously recorded up to step IV at 820 °C. It was predicted that in step II, some of PESf polymers would undergo imperfect decomposition resulting in deposited carbon. The deposited carbon would then be oxidized at 600-820 °C to form  $CO_2$  in step III and IV [20]. However, the percentage of weight loss in the PESf-related weight loss steps (II-IV) (10.28 %) was the larger than was expected based on the theoretical value calculation. This means that not only PESf, but also some parts of LSCF were removed during steps II-IV. This may be due to the oxidation of carbon/graphite that not only consumes oxygen from the atmosphere but also oxygen in the LSCF crystal lattice, leaving a reduced amount of LSCF 6428. However, further analysis revealed that there was an increase in weight at temperatures 820-1000 °C (step V) with the final weight being 5.66 mg. The increase in weight was caused by the adsorption of oxygen from the air by the

LSCF crystal lattice to reoxidize the oxygen vacancies in LSCF [13]. The total weight loss observed from 500-1000 °C was 9.00 %, which was similar to the theoretical value.

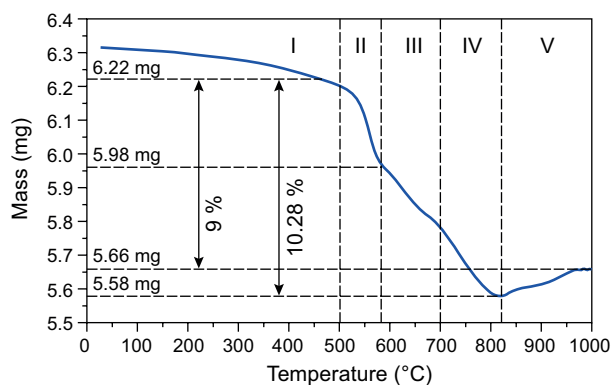


Figure 3. TGA curve of LSCF 6428 green membrane.

The slight difference between the theoretical value and the TGA result (0.12 %) might be attributed to the sluggish decomposition of PESf that may occur before 500 °C [20] [23]. The TGA results suggest that the sintering process for the green membrane should be carried out gradually so that the PESf polymer does not decompose rapidly, which causes damage to the pore structure. Thus, in this work, the sintering process was performed by holding the starting temperature for PESf decomposition at 500 °C for an hour, followed by holding the temperature at 700 °C for an hour to allow time for the decomposition of the carbon to occur.

#### Morphological analysis

SEM analysis was performed to examine the morphology of the perovskite membranes, at the dense and porous surfaces, as well as at the cross-section of the membrane. The analysis was conducted before, on the green membrane, and after sintering was performed (sintered membrane at each temperature). The SEM images of the green membrane are shown in Figure 4. It can be seen that for both surfaces (Figures 4a and b), the LSCF particles were uniformly distributed and

connected by the presence of the polymer binder [9]. It is also apparent that the membrane preparation procedure was successful in forming an asymmetric membrane, as shown through the presence of the porous and dense layers in the cross-section image (Figure 4c). The porous layer was dominated by finger-like pores, where the sponge-like pores were formed by the quick exchange between the solvent (DMSO) with DM water. The DM water replaced the DMSO as the DMSO was dissolved in the water, creating pores along its path in the microstructure of the membrane called finger-like pores [9, 13].

Figure 5 shows the morphology of membranes, which were sintered at various temperatures and durations. The sintering temperatures at 950 °C and 1100 °C were maintained for 4 and 8 hours, while the sintering at 1250 °C was conducted for 4 hours only. Sintering at 950 °C and 1100 °C for 4 hours produced membranes with high porosity and with an irregular surface morphology in the porous and dense layer as shown in Figures 5a and 5b. The formation of an asymmetric pore was not clearly observed for both membranes. However, the finger-like pores which present in the green membrane are still apparent. The irregular surface morphology and lack of clarity for the finger-like porous layer are possibly caused by the reduction in particles sintering after the removal of the polymer binder (PESf). Where the sintering temperatures of 950 and 1100 °C were not high enough to effectively sinter the membrane, causing only partial sintering of each LSCF particle, leaving an irregular pore structure as depicted in Figure 5a and Figure 5b. The results suggest that sintering at 950 and 1100 °C for 4 h is not sufficient to create a fine asymmetric membrane [10].

In contrast to membranes that were sintered at 950 and 1100 °C, those sintered at 1250 °C showed an increasingly regular surface morphology as can be seen in Figure 5c, where the LSCF particles on both surfaces were sintered and connected. The pore was still apparent on both porous and dense layer after sintering. However, the size and the number of pores found on the dense layer was much less than on the porous layer, indicating that the dense layer was indeed denser than the porous layer. Further examination of the cross-section is shown in Figure 5c, where the asymmetric membrane was formed.

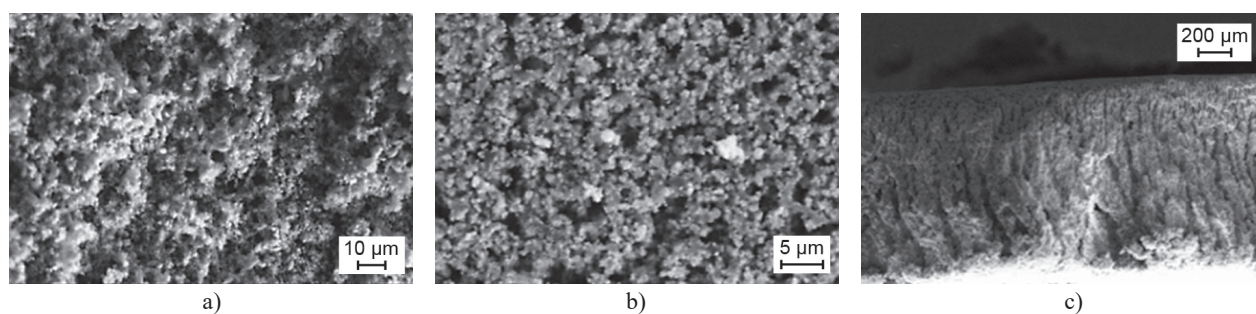


Figure 4. SEM images of green LSCF membrane: a) dense layer, b) pores layer and c) cross section.

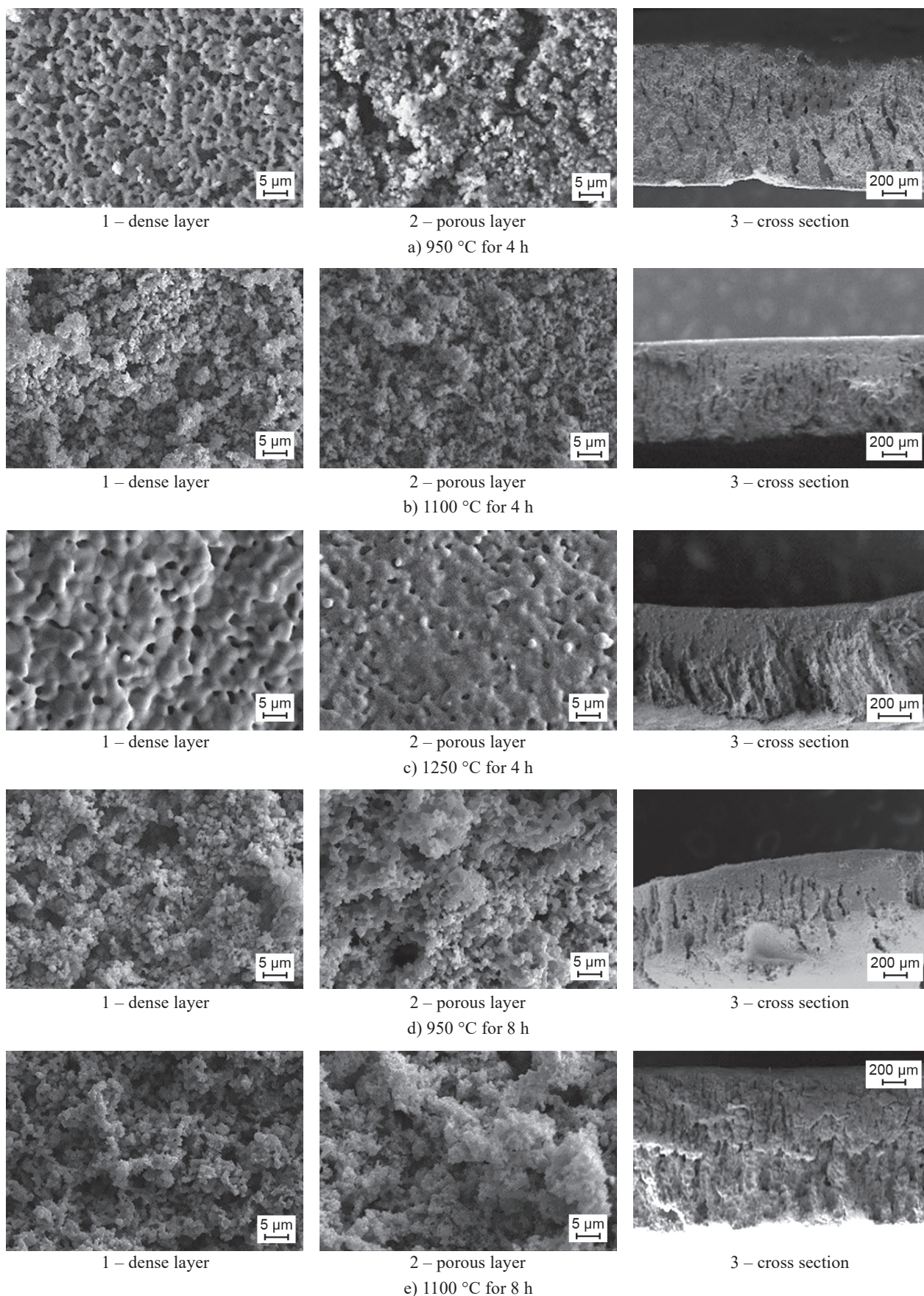


Figure 5. SEM images of sintered membranes at: a) 950 °C for 4 h, b) 1100 °C for 4 h, c) 1250 °C for 4 h, d) 950 °C for 8 h and e) 1100 °C for 8 h.

The sintered membrane at 1250 °C retains the finger-like pores of the green membrane, where the temperature is high enough to sinter the LSCF particles to form larger particles and reduce the size of the hole on the membrane surface.

#### Membrane shrinkage

The sintering process has been shown to promote membrane shrinkage due to the removal of holes in the green membranes. In this work, the degree of shrinkage was determined in terms of membrane thickness. The percentage of shrinkage depended on several factors such as particle size, amount of polymer binder, and sintering temperature [15]. Table 4 shows the shrinkage of the sintered membrane at various temperatures. It can be seen that the highest shrinkage percentage (55.88 %) occurs for membranes sintered at 1250 °C for 4 hours. The shrinkage observed at this temperature is in accordance with the SEM analysis. Whereby the shrinkage is due to sintering of the LSCF particles to form larger particles, which effectively also increases the density of the membrane [11]. For membranes sintered at 950 °C and 1100 °C, the increased sintering duration was associated with an increased shrinkage percentage. The sintering duration seems to have an effect on the compaction of the particle but the effect observed also less than that relating to the sintering temperature.

Table 4. Shrinkage of membranes sintered at various temperature.

Sintering condition	Length (mm)		Shrinkage (%)
	Initial	Final	
1250 °C, 4 h	17.0	7.5	55.88
1100 °C, 4 h	17.0	15.0	11.76
950 °C, 4 h	17.0	16.0	5.88
1100 °C, 8 h	17.0	10.0	41.17
950 °C, 8 h	17.0	12.0	29.41

To obtain a deeper understanding of the factors influencing membrane sintering, including sintering temperature and sintering duration, the membranes were also sintered at 950 and 1100 °C with a longer duration than before i.e. 8 h. The resulting morphology was then examined using SEM to compare any difference with the shorter sintering duration (4 h) at the same sintering temperature. The SEM image of membranes sintered at 950 and 1100 °C for 8 h is shown in Figure 5d and Figure 5e. The figures show that the membrane surfaces still possess irregular morphology on both the porous and dense layers. It seems that the sintering temperature has the greatest effect on the formation of the asymmetric membrane when compared with the sintering duration, whereby increased sintering temperatures were associated with the production of denser membranes.

In addition to shrinkage of the membranes, the porosity of the membranes was also examined. The porosity was approximated from the amount of water adsorbed by the membranes, whereby the more porous membrane will adsorb greater volumes of water. The results of the volume of water adsorbed by the membranes is tabulated in Table 5. The membrane associated with a sintering temperature of 1250 °C demonstrated the smallest amount of water adsorbed (0.07 ml·g<sup>-1</sup>). This is in accordance with the SEM results shown in Figure 5c, and the shrinkage trend, indicating that this membrane has the greatest density. Membranes sintered at 950 °C and 1100 °C for 4 hours were observed to adsorb a larger amount of water than those sintered at the same temperature for 8 hours. The results indicated that although there was apparently no significant change in the membrane morphology, the prolonged sintering duration may still produce denser membranes.

Table 5. Porosity of LSCF membranes determined by the water adsorption method.

Sintering condition	Pores volume (ml·g <sup>-1</sup> )
1250 °C, 4 h	0.07
1100 °C, 4 h	0.21
950 °C, 4 h	0.45
1100 °C, 8 h	0.13
950 °C, 8 h	0.25

#### Vickers hardness analysis

Vickers hardness analysis was also carried out to determine the strength of the sintered membranes. The membrane that was sintered at 1250 °C was the only sample to be tested as the others were too brittle to be tested. In this test, the membrane was indented at five different points on its surface with a load of 0.5 N and held for a period of 10 seconds for each test. The hardness recorded for each of the five indentation points was tabulated on Table 6, which shows that the average hardness of the membrane was 412.36 Hv. The hardness value was similar to that recorded for the symmetric membranes of Ba<sub>0.7</sub>Sr<sub>0.3</sub>Co<sub>0.8</sub>Fe<sub>0.2</sub>O<sub>3.8</sub> prepared by the dry pressing method [11]. However, the hardness at each

Table 6. Hardness value of sintered LSCF asymmetric membrane at 1250 °C.

Indentation point	Hv (Kgf·mm <sup>-2</sup> )	Hv average (Kgf·mm <sup>-2</sup> )
1	386.2	412.36
2	488.9	
3	456.4	
4	451.4	
5	278.9	

indentation point was varied, indicating that the hardness on the membrane was not uniform. This effect may be caused by the different morphology at each indentation point on the sample tested.

#### Thermal expansion coefficient analysis

The thermal expansion coefficient (TEC) is an important factor to consider for the perovskite membrane due to its function as an ionic transport mechanism for POM at high temperatures. The large mismatch between the membrane and reactor support, such as alumina, could lead to cracking in the membrane and/or ceramic sealant. Therefore, the TEC of the resulting asymmetric membranes were further tested using TMA (Thermal Mechanical Analyzer).

Figure 6 shows the TEC value of the sintered membrane at a different temperature of 950, 110 and 1250 °C. The results show that the sintered membrane at 950 °C was associated with the highest TEC value. These results are in accordance with previous reports [11] that found that the physical properties of membranes, especially the asymmetric ones, affect the TEC value. As the sintered structure leads to a change in density, which may provide different spaces within the membrane. In this case, the hole within the membranes could function as space for particles to be expended. Therefore, increased pores located on the membrane were associated with a higher TEC value [9]. In addition, some literature reports show that perovskite in powder form influenced the TEC value recorded [9, 11, 24]. However, in this work, the effect of this factor can be negated as the membranes were prepared from the same fine powder composition.

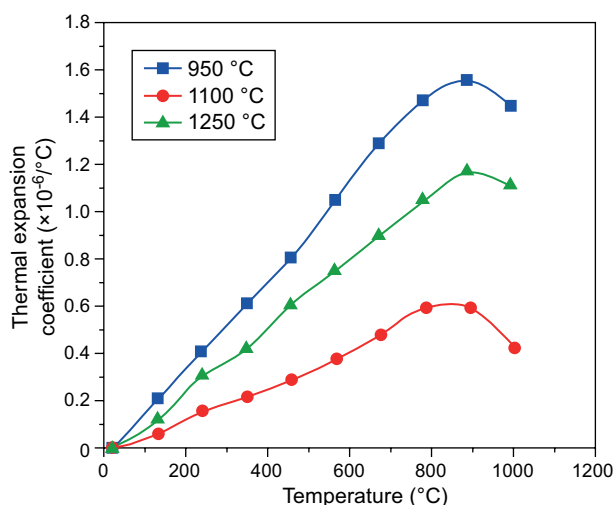


Figure 6. Thermal expansion coefficient of the asymmetric LSCF membrane at different sintering temperatures of 950, 1100 and 1250 °C.

## CONCLUSIONS

The asymmetric dense membrane of  $\text{La}_{0.6}\text{Sr}_{0.4}\text{Co}_{0.2}\text{Fe}_{0.8}\text{O}_{3-\delta}$  (LSCF) has been successfully prepared by the phase inversion method, followed by sintering. The membranes possess finger-like pores integrated with sponge-like pores. The morphology and mechanical properties of the membranes were observed to be affected by the sintering temperature. In addition, the sintering temperature 1250 °C showed the greatest density at the dense layer and a smaller hole on the membrane surface, with a clear asymmetric structure. Membranes that were sintered at 950 and 1100 °C showed decreased densities for both the dense and porous layers and an unclear asymmetric structure due to poor sintering. Higher temperatures were also found to cause greater shrinkage on the membranes, which influenced the associated hardness and thermal expansion coefficient. These analyses showed that the higher density and hardness of the membrane were correlated with lower TEC values.

## Acknowledgments

The authors would like to thank the Laboratory of the Chemistry of Materials and Energy and Laboratory of Energy and Environment ITS for supporting the authors with facilities and equipment to conduct this research. This research was funded by the Indonesian Ministry of Research, Technology and Higher Education under the PTP Grant scheme number 972/PKS/ITS/2018. S.D.N. received PMDSU research grant number 796/PKS/ITS/2018 while W.P.U. was funded by LPPM ITS under Penelitian Pemula (startup research) grant scheme with contract number 749/PKS/ITS/2017.

## REFERENCES

1. Teraoka Y., Zhang H.M., Furukawa S. Yamazoe N. (1985): Oxygen permeation through perovskite-type oxides. *Chemistry Letters*, 14, 1743–1746. doi: 10.1246/cl.1985.1743
2. Zeng P.C. (2007): Re-evaluation of  $\text{Ba}_{0.5}\text{Sr}_{0.5}\text{Co}_{0.8}\text{Fe}_{0.2}\text{O}_{3-\delta}$  Perovskite as Oxygen Semi-permeable Membrane. *Journal of Membrane Science*, 291, 148-156. doi: 10.1016/j.memsci.2007.01.003
3. Shelepova E., Vedyagin A., Sadykov V., Mezentseva N., Fedorova Y., Smorygo O., Klenov O. Mishakov I. (2016): Theoretical and experimental study of methane partial oxidation to syngas in catalytic membrane reactor with asymmetric oxygen-permeable membrane. *Catalysis Today*, 268, 103-110. doi: 10.1016/j.cattod.2016.01.005
4. Valderrama G., Kiennemann A., Goldwasser M. (2008): Dry reforming of  $\text{CH}_4$  over solid solutions of  $\text{LaNi}_{1-x}\text{Co}_x\text{O}_3$ . *Catalysis Today*, 133-135, 142-148. doi: 10.1016/j.cattod.2007.12.069
5. Jun Y., Meng X., Meng B., Yang N., Zhang C. (2016): Simulation of oxygen permeation through  $\text{La}_{0.6}\text{Sr}_{0.4}\text{Co}_{0.2}\text{Fe}_{0.8}\text{O}_{3-\delta}$  tubular membrane reactor with POM reactions. *International Journal Hydrogen Technology*, 41, 17399-17407. doi: 10.1016/j.ijhydene.2016.07.076

6. Chi Y., Li T., Wang B., Wu Z., Li K. (2017): Morphology, performance and stability of multi-bore capillary  $\text{La}_{0.6}\text{Sr}_{0.4}\text{Co}_{0.2}\text{Fe}_{0.8}\text{O}_{3-\delta}$  oxygen transport membranes. *Journal of Membrane Science*, 529, 224-233. doi: 10.1016/j.memsci.2017.02.010
7. Ren J., Zhou J., Deng M. (2010): Morphology Transition of Asymmetric Flat Sheet And Thickness-Gradient Membranes By Wet Phase-Inversion Process. *Desalination*, 253, 1-8. doi: 10.1016/j.desal.2009.12.001
8. Mulder M. (1992). *Basic Principles of Membrane Technology*, Kluwer Academic Publishers.
9. Tan X., Liu Y., Li K. (2005): Preparation of LSCF Ceramic Hollow-Fiber Membranes for Oxygen Production by a Phase-Inversion/Sintering Technique. *Industrial & Engineering Chemistry Research*, 44, 61-66. doi: 10.1021/ie040179c
10. Setyaningsih E. P., Machfudzoh M., Utomo W. P., and Fansuri, H. (2016): Preparation of  $\text{CaTiO}_3$  Asymmetric Membranes Using Polyetherimide as Binder Polymer. *Indonesian Journal of Chemistry*, 16, 20-24. doi: 10.22146/ijc.21172
11. Fansuri H., Syafi'i M.I., Romdoni S., Masyitoh A.D., Utomo W.P., Prasetyoko D., Widiastuti N., Murwani I.K., Subaer (2017): Preparation of dense  $\text{Ba}_x\text{Sr}_{1-x}\text{Co}_{0.8}\text{Fe}_{0.2}\text{O}_3$  membranes: Effect of  $\text{Ba}^{2+}$  substituents and sintering method to the density, hardness and thermal expansion coefficient of the membranes. *Advanced Materials Letters*, 8, 799-806. doi: 10.5185/amlett.2017.6948
12. Utomo W.P., Aliyatulmuna A., Fansuri H. (2013): Oxygen Permeability of LSCF 7382, SCF 182 and BSCF 5582 Asymmetric Membranes, 8<sup>th</sup> International Student Conference on Advanced Science and Technology (8<sup>th</sup> ICAST). Kumamoto, Japan, 12-13 December 2013.
13. Xie H., Zhuang L., Chen Y., Wang H. (2017): Phase-inversion synthesize of asymmetric-structured  $\text{La}_{3.5}\text{W}_{0.6}\text{Mo}_{0.4}\text{O}_{11.25-\delta}$  membranes with enhanced hydrogen permeation flux. *Journal of Alloys and Compounds*, 729, 890-896. doi: 10.1016/j.jallcom.2017.09.221
14. Nurherdiana S. D., Sholichah N., Iqbal R.M., Sahasrikirana M., Utomo W. P., Akhlus S., Nurlina Fansuri H. (2017): Preparation of  $\text{La}_{0.7}\text{Sr}_{0.3}\text{Co}_{0.2}\text{Fe}_{0.8}\text{O}_{3-\delta}$  (LSCF 7328) by Combination of Mechanochemical and Solid State Reaction. *Key Engineering Materials*, 744, 399-403. doi: 10.4028/www.scientific.net/KEM.744.399
15. Wang Z., Yang N., Meng B., Tan X. (2009): Preparation and Oxygen Permeation Properties of Highly Asymmetric  $\text{La}_{0.6}\text{Sr}_{0.4}\text{Co}_{0.2}\text{Fe}_{0.8}\text{O}_{3-\delta}$  Perovskite Hollow Fiber Membranes. *Industrial Engineering & Chemistry Research*, 48, 510-516. doi: 10.1021/ie8010462.
16. Mineshige A., Izutsu J., Nakamura M., Nigaki K., Abe J., Kobune M., Fujii S., Yazawa T. (2005): Introduction of A-site deficiency into  $\text{La}_{0.6}\text{Sr}_{0.4}\text{Co}_{0.2}\text{Fe}_{0.8}\text{O}_{3-\delta}$  and its effect on structure and conductivity. *Solid State Ionics*, 176, 11451149. doi: 10.1016/j.ssi.2004.11.021
17. Hjalmarsson, P., Sogaard, M., Hagen, A., Mogensen, M. (2008): Structural Properties and Electrochemical Performance of Strontium- and Nickel-substituted Lanthanum Cobaltite. *Solid State Ionics*, 179, 636-646. doi: 10.1016/j.ssi.2008.04.026
18. Kivi I., Aruväli J., Kirsimäe K., Heinsaar A., Nurk G., Lust E. (2013): Changes in LSC and LSCF Cathode Crystallographic Parameters Measured by Electrochemical in situ High-Temperature XRD. *ECS Transactions*, 57, 1841-1849. doi: 10.1149/05701.1841ecst
19. Hashimoto S., Fukuda Y., Kuhn M. Sato K., Yashiro K., Mizusaki J. (2011): Thermal and chemical lattice expansibility of  $\text{La}_{0.6}\text{Sr}_{0.4}\text{Co}_{1-y}\text{Fe}_y\text{O}_{3-\delta}$  ( $y = 0.2, 0.4, 0.6$  and  $0.8$ ). *Solid State Ionics*, 186, 37-43.
20. Yuan R., He W., Zhang Y., Gao J., Chen C. (2016): Preparation and characterization of supported planar  $\text{Zr}_{0.84}\text{Y}_{0.16}\text{O}_{1.92}-\text{La}_{0.8}\text{Sr}_{0.2}\text{Cr}_{0.5}\text{Fe}_{0.5}\text{O}_{3-\delta}$  composite membrane. *Journal of Membrane Science*, 499, 335-342. doi: 10.1016/j.memsci.2015.10.066
21. Qiu Z., Hu Y., Tan X., Hashim S.S., Sunarso J., Liu S. (2018): Oxygen Permeation Properties of Novel  $\text{BaCo}_{0.85}\text{Bi}_{0.05}\text{Zr}_{0.1}\text{O}_{3-\delta}$  Hollow Fibre Membrane. *Chemical Engineering Science*, 177, 18-26. doi: 10.1016/j.ces.2017.11.006
22. Nasir R., Mukhtar H., Man Z. (2014): Fabrication, Characterization and Performance Study of M-methyl-diethanolamine (MDEA)-Polyethersulfone (PES) Amine Polymeric Membrane for  $\text{CO}_2/\text{CH}_4$  Separation. *Journal of Applied Sciences*, 14, 1186-1191. doi: 10.3923/jas.2014.1186.1191
23. Velu S., Muruganandam L., Arthanareeswaran G. (2015): Preparation And Performance Studies on Polyethersulfone Ultrafiltration Membranes Modified with Gelatin for Treatment of Tannery and Distillery Wastewater. *Brazilian Journal of Chemical Engineering*, 32, 179-189. doi: 10.1590/0104-6632.20150321s00002965
24. Aliyatulmuna A., Utomo W.P., Burhan R.Y.P., Fansuri H., Murwani I.K. (2017): Thermal Expansion, Microhardness and Oxygen Permeation of  $\text{La}_{1-x}\text{Sr}_x\text{Co}_{0.8}\text{Fe}_{0.2}\text{O}_{3-\delta}$  Membranes. *Asian Journal of Chemistry*, 29, 2191-2196. doi: 10.14233/ajchem.2017.20681